



Sensors and Actuators B: Chemical
Volume 165, Issue 1, April 2012, Pages 143-150



Use of nanohybrid materials as electrochemical transducers for mercury sensors

Daniel Martín-Yerga, María Begoña González-García, Agustín Costa-García  

 **Show more**

<https://doi.org/10.1016/j.snb.2012.02.031>

[Get rights and content](#)

This is a preprint manuscript. Please, download the final and much nicer version at:

<https://doi.org/10.1016/j.snb.2012.02.031>

USE OF NANOHYBRID MATERIALS AS ELECTROCHEMICAL TRANSDUCERS FOR MERCURY SENSORS

Daniel Martín-Yerga, María Begoña González-García, Agustín Costa-García*

Departamento de Química Física y Analítica, Universidad de Oviedo, C/ Julián Clavería, 8, 33006, Oviedo, Spain

Abstract

The electrochemical behavior of mercury using different nanostructured screen-printed transducers has been studied. The first underpotential deposition (UPD) was chosen as the best electrochemical process to detect low amounts of mercury on gold nanostructured electrodes. Several nanostructured electrochemical transducers using carbon nanotubes, graphene oxide and gold nanoparticles were generated, characterized and optimized for mercury determination in water. The transducer with a nanohybrid surface of carbon nanotubes and gold nanoparticles was the best suited to solve the analytical problem. For this sensor, a calibration plot from 0.5 to 50 $\mu\text{g/L}$ was obtained in acidic solutions of Hg(II) with an intraelectrode reproducibility of 3% ($n = 5$). The detection limit was 0.2 $\mu\text{g/L}$ of mercury. The performance of the sensor was then evaluated using real samples of tap and river water with good accuracy.

Keywords: *Nanohybrid transducer, Underpotential deposition, Mercury sensor, Carbon nanotubes, Gold nanoparticles, Screen-printed carbon electrode.*

1. Introduction

Mercury is considered one of the most dangerous chemical pollutants, and, unfortunately, it is one of the most abundant heavy metals in the environment. It is widely distributed in air, water and soil. Although the use of mercury is being reduced in all possible areas, still 2000 t are emitted annually from anthropogenic sources[1]. The toxicity of mercury varies with its chemical form, but all mercury species are toxic. It can be accumulated in some vital organs as the liver, heart, brain and tissues as bones. Exposition to mercury can cause kidney failure, nervous system disorders, intellectual impairment and even death[2]. Therefore, mercury analysis in water is essential to prevent issues for human beings and the environment.

* Corresponding author. Tel.: + 34 98 510 34 88
E-mail address: costa@uniovi.es (Agustín Costa García)

GO: Graphene Oxide

SPCnAuEs: Screen-Printed Carbon/Gold Nanoparticles Electrodes

SPCNTnAuEs: Screen-Printed Carbon Nanotubes/Gold Nanoparticles Electrodes

SPGOnAuEs: Screen-Printed Graphene Oxide/Gold Nanoparticles Electrodes

29 The most used analytical methods for mercury determination are cold vapor atomic fluorescence
30 spectroscopy(CVAFS)[3],cold vapor atomic absorption spectroscopy (CVAAS)[4] and, also, ICP-
31 MS[5]. These methods have an expensive instrumentation, with complex sample preparation and
32 cannot be used for in-situ analysis. The search for a fast, cheap, simple and easily portable
33 methodology that allows performing an in-situ analysis of the environment samples is a constant
34 concern. Hence, electrochemical analysis due to their excellent sensitivity, short analysis time, and
35 cheap instrumentation is a good alternative to solve those challenges. Within this field, anodic
36 stripping voltammetry (ASV) using gold electrodes has shown its applicability and has even been
37 recommended by the US Environmental Protection Association (EPA) for the quantification of heavy
38 metals as mercury[6].

39 Gold is an excellent material as a working electrode because it has high affinity for mercury
40 enhancing thepreconcentration effect[7,8]. In addition, some metals such as mercury, arsenic, or lead
41 present a process called underpotential deposition (UPD)[9]. The UPD is a fundamental
42 electrochemical process andhave attracted a long-standing interest. It happens by the strong
43 interaction between the metal and the gold electrode after the reduction of ionic metal, resulting in the
44 formation of an adlayer. In the case of mercury, this process is of particular importance due to its
45 special electrochemical properties and the amalgam formation.Several types of gold electrodes have
46 been used for the electrochemical determination of mercury, such as gold disk[10], gold film[11], gold
47 microelectrode arrays[12], and gold fiber[13]. This kind of electrodes, generally, employs
48 instrumentation still intended for laboratory use and thus unsuitable for in-situ analysis.

49 The research on chemical sensors has grown exponentially in recent years, because these devices
50 haveideal characteristics such as low cost, possibility of miniaturization and ease of use, allowing their
51 use for in-situ analysis by non-specialist personal. Among the tools for the design of chemical
52 sensors, the screen-printed electrodes (SPEs) stand out, since these devices fulfill many of the ideal
53 characteristics of electrochemical sensors. Many applications have been resolved using screen-
54 printed electrodes in sensor and biosensor technology[14]. Gold based screen-printed electrodes
55 have been employed for mercury determination in water[15]or fish samples[16].

56 The excellent properties of nanomaterials can be exploited to solve analytical problems more
57 efficiently than to date. Nanomaterials are especially interesting for its application to electrochemical
58 sensors, producing beneficial effects such as increased mass transport and electron transfer, catalytic
59 activity, and enhancement of the analytical signal due to its high volume-surface relation. Among the
60 most widely used nanomaterials in electrochemical analysis are metal nanoparticles[17,18] and
61 carbon nanotubes[19]. In the last years, different nanomaterials have been employed for
62 electrochemical biosensors such as gold nanoparticles[20], carbon nanotubes[21] and graphene[22].
63 Forthe electrochemical determination of mercury, gold nanoparticlesare a promising electrode
64 material, as it combines its properties as nanomaterial and the high affinity for mercury.In fact, glassy
65 carbon electrodes have been employed for mercury analysis modified with different nanomaterials
66 such as gold nanoparticles[23], carbon nanotubes[24], and nanohybrids such as gold
67 nanoparticles/carbon nanotubes[25] or gold nanoparticles/graphene[26].

68 Screen-printed electrodes can be easily modified with different nanomaterials so that after the
69 modification is possible the resolution of new analytical problems. Modification of SPEs with
70 nanomaterials has been previously studied by our group. For instance, Martínez-Paredes et
71 al.[27] studied several methodologies for the modification of SPEs with gold nanoparticles and the best
72 results were obtained using an electrochemical method. With this methodology the nanoparticles can
73 be optimized for a particular application, with a controllable diameter. Furthermore, the distribution of
74 the generated nanoparticles is fairly homogeneous forming an array-type electrode. For modification
75 with carbon nanotubes, the most significant problem is the efficient dispersion of the nanotubes in
76 solution. Fanjul-Bolado et al. developed a method with good results for the modification of SPEs with
77 carbon nanotubes[28].

78 Screen-printed carbon electrodes modified with gold nanoparticles have been employed for the
79 determination of many analytes such as lead[29] or chromium[30], and for application to geno-[31] and
80 immunosensors[32]. Also, carbon nanotubes are useful for modification of SPEs, resolving some
81 problems such as p-aminophenol determination[33]. A gold film on screen-printed carbon electrodes
82 has been used for mercury and lead determination in tap water after preconcentration with magnetic
83 particles[34]. Due to the excellent properties of those nanostructures, the modification of SPEs with
84 nanohybrid materials is a current trend [35]. This is an innovative technology and is starting to be
85 used to solve important clinical problems such as the detection of celiac disease[36].

86 In this work, we propose an original methodology using different nanohybrid materials on screen-
87 printed carbon electrodes as electrochemical transducers for the construction of chemical sensors for
88 mercury determination in water.

89 **2. Experimental**

90

91 **2.1. Apparatus and electrodes**

92 Voltammetric measurements were performed with an Autolab PGSTAT 12 (Eco Chemie, The
93 Netherlands) potentiostat/galvanostat interfaced to an AMD K6 266 MHz computer system and
94 controlled by Autolab GPES 4.9. All measurements were carried out at room temperature.

95 Screen-printed carbon electrodes (SPCEs) were purchased from DropSens (Spain). These electrodes
96 incorporate a conventional three-electrode configuration, printed on ceramic substrates (3.4 x 1.0 cm).
97 Both working (disk-shaped 4 mm diameter) and counter electrodes are made of carbon inks, whereas
98 pseudoreference electrode and electric contacts are made of silver. An insulating layer was printed
99 over the electrode system, leaving uncovered the electric contacts and a working area which
100 constitutes the reservoir of the electrochemical cell, with an actual volume of 50 μL . Screen-printed
101 gold electrodes (SPAuEs) were also purchased from DropSens and have the same design than those
102 of carbon, but in this case, working and counter electrodes are made of gold paste cured at low

103 temperature. The SPEs were connected to the potentiostat through a specific connector (DropSens,
104 ref. DSC).

105 A JEOL 6610LV scanning electron microscope (30 kV, Japan) was used to characterize the working
106 electrodes. An Elmasonic P ultrasonic bath (Elma GmbH, Germany) was also employed.

107 An Element Finnigan MAT instrument was used for ICP-MS as the reference technique for the
108 analysis of mercury using a standard protocol.

109 2.2. Reagents and solutions

110 Standard gold (III) tetrachloro complex was purchased from Merck (1.000 ± 0.002 g of
111 tetrachloraurate(III) in 500 mL 1.0 M HCl). Carboxyl modified multiwalled carbon nanotubes
112 (MWCNTs) were purchased from Nanocyl (Belgium, ref. 3151). Graphene oxide (GO) was kindly
113 provided by Nanoinnova Technologies (Spain). Mercury acetate was purchased from Fluka (> 99.0 %
114 purity). Lead nitrate, fuming hydrochloric acid (37.0 %), N,N-dimethylformamide (DMF) (99.8 %) and
115 standard solutions of Cd(II), Se(IV) and Zn(II) (1000 mg/L) were purchased from Merck. Stock
116 solutions of Hg(II) and Pb(II) (0.50 g/L) were prepared in 0.10 M hydrochloric acid. Copper sulfate was
117 purchased from Probus. Ultrapure water obtained with a Millipore Direct Q5™ purification system
118 from Millipore Ibérica S.A. (Madrid, Spain) was used throughout this work. All other reagents were of
119 analytical grade.

120 Drinking water samples were collected from a running water tap in our lab at the Department of
121 Physical and Analytical Chemistry, University of Oviedo. River water samples were collected from
122 Arlos River located in Llaranes (Asturias, Spain).

123 MWCNTs solution was prepared by mixing 1.0 mg of MWCNT-COOH with 1.0 ml of a mixture
124 DMF:water (1:1) by sonication using an ultrasonic bath for 2 h. A dilution of this solution was made for
125 a final concentration of 0.10 g/L by sonication for 30 minutes. GO solutions were made in water using
126 the same procedure. Diluted solutions of gold tetrachloroaurate and mercury acetate were prepared
127 by suitable dilution with 0.10 M hydrochloric acid.

128 2.3. Procedures

129

130 2.3.1. Modification of screen-printed electrodes with nanomaterials

131 Gold nanostructures were generated in-situ over SPCEs (SPCnAuEs) following a method developed
132 by Martínez-Paredes et al.[27]. It consists in dropping an aliquot of 40 μ L of an acidic solution of
133 AuCl_4^- on the electrode surface and applying a constant current intensity for a specific period of time.

134 Modification of SPEs with carbon nanotubes was carried out following a method developed by Fanjul-
135 Bolado et al.[28]. It consists in depositing an aliquot of 4 μ L of the MWCNT-COOH dispersion (0.10
136 g/L in DMF:water) on the working electrode surface. The solution was left to dry at room temperature

137 (20 °C) until its absolute evaporation. Modified electrodes were carefully washed with water and dried
138 at room temperature.

139 Modification of SPEs with graphene oxide was carried out depositing an aliquot of 10 μ L of the
140 graphene oxide dispersion (0.10 g/L in water) on the working electrode surface. The solution was left
141 to dry at room temperature (20 °C) until its absolute evaporation. Modified electrodes were carefully
142 washed with water and dried at room temperature.

143 In this work, two different nanohybrid transducers (SPGOnAuEs and SPCNTnAuEs) were prepared.
144 Those transducers were prepared modifying the working electrode with GO or MWCNTs respectively,
145 followed by gold nanostructuring using the explained procedures. This method has been previously
146 used for modification of SPEs with nanohybrid materials by Neves et al.[35].

147 2.3.2.Characterization of the gold nanostructured sensors

148 Gold nanostructures were characterized by SEM and by chronoamperometry. For the optimized
149 sensors (SPCnAuEs, SPGOnAuEs and SPCNTnAuEs), SEM images were obtained and the mean
150 diameter of the gold nanoparticles was measured.Chronoamperometry measurements were
151 performed to determine the amount of gold deposited on the different sensors. An aliquot of 40 μ L of
152 0.10 M HCl was dropped onto the electrode and the oxidation of gold was carried out by holding the
153 electrode at a potential of +0.85 V, recording the current intensity vs. time. Three electrodes were
154 measured for each kind of sensor. The area under the curve (charge) was used to calculate the mass
155 of gold involved in the process using the Faraday equation.

156 2.3.3.Voltammetric measurements of mercury

157 Mercury was preconcentrated over the sensor by applying a constant potential of +0.30 V for a period
158 of time optimized for every different transducer. Then, the potential is switched between +0.30 V and
159 +0.55 V using square-wave voltammetry (SWV), at a frequency, amplitude and step potential
160 optimized for every transducer. All measurements were performed without removing oxygen from the
161 solution, and using an aliquot of 40 μ L of the appropriate solution.

162 Voltammograms obtained for mercury on gold, generally, have a broad baseline. This is consistent
163 with data obtained by other authors as Welch et al. [37] and due to this for low concentrations is
164 difficult to measure the peak height. For this kind of voltammograms, the GPES software has a tool to
165 get a more defined peak and therefore to measure its height in an easier way. This tool is called
166 "Baseline correction" and is located in the "Edit data" menu of the GPES software. This treatment was
167 done to the voltammograms obtained for the calibration plots, and then the peak height was
168 measured more accurately.

169 2.3.4.Simultaneous voltammetric measurements of mercury and lead

170 Mercury and lead were preconcentrated over the sensor by applying a constant potential of -0.55 V
171 for 120 s. Then, the potential is switched between -0.55 V and +0.55 V using square-wave

172 voltammetry, at a frequency of 50 Hz, amplitude of 25 mV and a step potential of 4 mV. All
173 measurements were performed without removing oxygen from the solution, and using an aliquot of 40
174 μL of the appropriate solution.

175 **3. Results and discussion**

176

177 **3.1. Electrochemical behavior of mercury**

178 Mercury behavior on different electrode surfaces was studied using cyclic voltamperometry (Fig. 1).
179 For SPCEs (Fig. 1A), two cathodic processes at potentials of -0.30 (C_5) and -0.62 V (C_B) were
180 observed. The -0.62 V process occurs in the blank solution, therefore it is not caused by mercury,
181 while the other process corresponds to the bulk deposition of mercury on SPCEs. An anodic stripping
182 peak appears at a potential of $+0.03$ V (A_5), which corresponds to the reoxidation of mercury.

183 For SPAuE (Fig. 1B) and SPCnAuEs (Fig. 1C) cases, it can be observed other mercury processes at
184 potentials more positive than the bulk deposition and its corresponding stripping process on SPCEs.
185 In both cases, 5 cathodic peaks are observed (SPAuEs: -0.20 V (C_5), -0.06 V (C_4), $+0.02$ V (C_3),
186 $+0.25$ V (C_2), $+0.42$ V (C_1); SPCnAuEs: -0.23 V (C_5), -0.05 V (C_4), $+0.03$ V (C_3), $+0.32$ V (C_2), $+0.47$ V
187 (C_1)). For SPAuEs, 4 anodic peaks were observed ($+0.00$ V (A_5), $+0.07$ V (A_n), $+0.23$ V (A_2), $+0.43$ V
188 (A_1)), while for SPCnAuEs, 5 anodic peaks were observed ($+0.01$ V (A_5), $+0.05$ V (A_4), $+0.15$ V (A_3),
189 $+0.30$ V (A_2), $+0.48$ V (A_1)). It is likely that in the case of SPAuEs, two of the anodic peaks perfectly
190 observed in SPCnAuEs (A_3 , A_4) are overlapped (A_n). Another visible difference is that the cathodic
191 processes for SPCnAuEs occur to slightly more positive potentials than for SPAuEs. This behavior
192 could be explained due to the bigger catalytic activity of gold nanoparticles, and therefore the
193 preconcentration of mercury on the electrode occurs more easily. Using SPCnAuEs and
194 SPGOnAuEs transducers, the behavior is similar to the obtained with SPCnAuEs. The observation of
195 5 redox processes for the mercury preconcentration on gold electrodes is consistent with those
196 obtained in other works, such as the one realized by Herrera et al.[38].

197 The two peaks appearing at more positive potentials (C_1 and C_2) in the presence of gold correspond
198 to the formation of a monolayer of atoms of mercury on the gold substrate at more positive potentials
199 than the reversible potential of Nernst for the formation of bulk metal, referred to as underpotential
200 deposition (UPD).

201 There are other processes besides the UPD ones and the bulk deposition. These are due to different
202 redox processes of mercury, which are probably influenced by the presence of Cl^- ions[39].

203 UPD processes are comparable to an adsorption process where the mercury is adsorbed and
204 reduced on gold at various stages. The presence of gold promotes the adsorption of mercury atoms
205 on the surface, produces a mercury reduction thermodynamically more favorable, and therefore, the
206 mercury reduction potential shifts to more positive potentials. The equivalent oxidation process also

207 requires a more positive potential because the stripping of the adsorbed mercury on gold will be more
208 difficult.

209 Voltammogram for SPAuEs and SPCnAuEs at the potentials where occurs the first UPD process (C_1
210 and A_1 processes) is shown in Fig. 2A. It can be observed as the peak intensity in the case of
211 SPCnAuEs (continuous line) is higher than for SPAuEs (dashed line) for the same
212 mercury concentration. Hence, the use of gold nanoparticles as electrode surface improves the
213 analytical signal produced. This may be due to the bigger surface area of the nanoparticles and the
214 array-type arrangement on the carbon surface. Then, the use of gold nanoparticles is more suitable
215 for the determination of mercury.

216 Cyclic voltammograms for two different concentrations of mercury on SPCnAuEs are shown in Fig.
217 2B. For the case of low concentrations (dashed line), only the first UPD is observed, whereas for a
218 higher concentration (continuous line), both UPD processes are observed. The second UPD only
219 occurs when the first UPD is saturated, therefore for low concentrations of mercury (normally for
220 uncontaminated and low-contaminated environmental samples) only the first UPD occurs. Thus, the
221 first UPD process is best suited for use in the determination of very low amounts of mercury.

222 The variation of the intensity of the first UPD peak with the scan rate of the cyclic voltammetry was
223 studied. Both the cathodic and corresponding anodic stripping peaks of the first mercury UPD were
224 linear with scan rate, according to the following equations:

225 Cathodic peak: $i_p (\mu A) = 0.009v (mV/s) + 0.510, R^2 = 0.997$

226 Anodic stripping peak: $i_p (\mu A) = 0.012v (mV/s) + 0.692, R^2 = 0.993$

227 According to this behavior can be suggested that the UPD is a process controlled by adsorption, as is
228 described in previous works[40].

229 Moreover, it was observed that the peak separation (ΔE_p) between the anodic and cathodic peaks in
230 SPCEs and SPCnAuEs were 330 and 10 mV (first UPD), respectively. This improvement in the
231 electrochemical performance is due to the strong interaction between mercury and gold, and to the
232 beneficial properties of gold nanoparticles.

233

234 Due to the behavior of the first UPD process, it can be used for the determination of very low mercury
235 concentrations when combined with anodic stripping voltammetry after a preconcentration step on the
236 working electrode. Besides, the use of gold nanoparticles on SPCEs improves the analytical signal,
237 showing clear advantages for its use instead of SPAuEs.

238

239 3.2.

Study of different

240 nanostructured transducers for mercury determination

241 Several gold nanostructures on SPCEs, SPCNTEs and SPGOEs were studied in order to obtain the
242 most suitable nanostructured sensor for mercury analysis. Thus, different sensors were fabricated
243 with gold nanoparticles generated under different experimental conditions (current, deposition time
244 and AuCl_4^- concentration). The analytical signal for 50 $\mu\text{g/L}$ of mercury was measured using each
245 fabricated sensor. The highest analytical signals were obtained using -100 μA of current, a deposition
246 time of 180 s, and a concentration of AuCl_4^- of 1.0mM(data not shown).

247 The different electrode surfaces generated by the optimized experimental conditions were
248 characterized by scanning electronic microscopy (SEM), and the amount of gold was calculated by
249 chronoamperometry. The data obtained is summarized in Table 1 and SEM images are shown in Fig.
250 3.

251 In the SEM images the gold nanoparticles appear as brighter spots than the carbon surface. Both the
252 dispersion and the size of the gold nanoparticles are different for each different sensor (SPCnAuEs,
253 SPCNTnAuEs and SPGOnAuEs), although the experimental conditions in which these nanoparticles
254 were generated were the same. For SPCNTnAuEs, the electrode is covered by two groups of gold
255 nanoparticles with a different mean diameter, whereas in the case of SPGOnAuEs, there are three
256 groups of nanoparticles. One of the groups has a greater number of nanoparticles. The difference in
257 diameters and groups of gold nanoparticles can be explained due to that the generation of the
258 nanoparticles is performed on the different carbon materials. These materials (carbon, carbon
259 nanotubes and graphene oxide) results in different electrodic surfaces where the nucleation and
260 growth of the gold nanoparticles will be different.

261 This fact indicates that the carbon surface where the nanoparticles are electrochemically generated
262 affects the size, dispersion and amount of gold nanoparticles. Therefore, depending on the
263 application, the experimental conditions of the generation of the gold nanoparticles must be optimized
264 for each different material of the working electrode.

265 3.3. Analytical response for the different transducers

266 The variable parameters for the analysis were optimized to find the most suitable to solve the issue of
267 the sensible mercury determination. Different electrolytic mediums were studied by Giacomino et
268 al.[41], and concluded that HCl was the most appropriate. Other authors have shown that a constant
269 concentration of Cl^- ions is important for mercury analysis[42]. Therefore, HCl was chosen as the
270 electrolytic medium and a study of several concentrations of HCl (0.01, 0.05, 0.10 and 0.50 M) was
271 carried out. The analytical signal for 50 $\mu\text{g/L}$ of mercury was measured, and the highest signal was
272 obtained with a concentration of 0.10 M. Giacomino et al. also concluded that the square wave
273 voltammetry technique was the most suitable for stripping of the deposited mercury. The UPD
274 process has a good reversibility (as shown in Fig. 2B), so the characteristics of the square wave
275 voltammetry technique can improve the sensitivity of the analytical signal. Thus, in this work, SWV
276 was used as the stripping technique.

277 The deposition potential was set to +0.30 V because more negative potentials could produce the
278 second UPD process or even the bulk deposition and using more positive potentials the analytical
279 signal decreases. Thus, using +0.30 V, only was observed an anodic peak at approximately +0.43 V,
280 due to the stripping of the deposited mercury on the gold nanoparticles.

281 According to some authors, the major drawback of gold electrodes is the well-known phenomenon of
282 structural changes of their surface, caused by amalgam formation[43,44]. Hence, in many of the
283 works where mercury is electrochemically determined is necessary a pretreatment to the electrode
284 before the analysis[37,45]. Inukai et al. described that it only happens when bulk deposition takes
285 place[46]. In our work, employing gold nanoparticles and the first UPD process, it was not necessary
286 any pretreatment before measurements. Despite the disposable character of these electrodes, when
287 the mercury is present in a simple matrix, the electrode can be reused rinsing it with water between
288 each measurement.

289 Other parameters as the deposition time, frequency, amplitude and potential step of the square wave
290 were optimized for each nanostructured sensor. Measurements of 20 $\mu\text{g/L}$ Hg (II) standard solution in
291 HCl 0.10M were made and the obtained signal was evaluated. The criterium for selecting the
292 optimized value was the evaluation of the peak height of the analytical signal. The optimized values
293 for deposition time, frequency, amplitude and potential step for the SPCnAuEs sensor were: 240 s, 80
294 Hz, 30 mV and 4 mV, respectively. For the SPCNTnAuEs and SPGOnAuEs sensors were: 200 s, 40
295 Hz, 20 mV and 8 mV, respectively.

296 With the optimized methodology, calibration plots were obtained for mercury using each fabricated
297 sensor (SPCnAuEs, SPGOnAuEs, SPCNTnAuEs). The calibration plot and the corresponding
298 voltammograms (after the baseline correction process explained in section 2.3.3) for the SPCNTnAuE
299 sensor are shown in Fig. 4.

300 Table 2 show different analytical data such as the linear range, slope of the calibration plots as well as
301 the detection limits (calculated as the concentration corresponding to a signal that is three times the
302 standard deviation of the intercept) and interelectrode reproducibility for each kind of sensor.
303 Although all sensors are able to detect low concentrations of mercury, there are significant differences
304 in the characteristics obtained for each one.

305 With this data, it was observed that the use of nanohybrid materials as electrodic surface, in
306 comparison with SPCnAuEs, improves considerably the linear range and the limit of detection. This
307 improvement may be due to the fact that the electrodic surface in these sensors consists entirely of
308 nanomaterials with the advantages that it entails, since both the carbon nanotubes and
309 grapheneoxide completely covers the working electrode and the previous carbon electrode only works
310 as an electrical contact. The obtained sensitivity (slope of the calibration plot) for the SPCNTnAuE
311 sensors was clearly higher to the obtained for SPCnAuEs. The lowest sensitivity was obtained for the
312 SPGOnAuE sensors. For SPCnAuEs, the saturation of the first UPD appeared to a higher
313 concentration. This data is consistent with the amount of gold available on the different sensors (Table

314 1). Moreover, it was obtained the intraelectrode reproducibility with similar values for each sensor: 8.5
315 % (SPCnAuEs), 11.4 % (SPCNTnAuEs) and 9.4 % (SPGOnAuEs) (eight repeated measurements for
316 50, 10 and 20 $\mu\text{g/L}$ of mercury, respectively).

317 The best analytical characteristics were presented by the nanohybrid sensor fabricated with carbon
318 nanotubes and gold nanoparticles (SPCNTnAuEs), since the detection limit of $0.2\mu\text{g/L}$ is lower than
319 that obtained with the other developed sensors, and moreover the sensitivity is better. Also, the linear
320 range for this sensor is wider, reaching two orders of magnitude. Even, the
321 interelectrode reproducibility is excellent, presenting a small deviation, the use of different sensors is
322 not going to change too much the results obtained.

323 The analytical characteristics that the SPCNTnAuE sensor offers, allow carrying out an analysis of
324 mercury in water because it fulfill the requirements of the guidelines set by WHO ($6.0\mu\text{g/L}$)[47], and
325 also different regulations of the water quality for human consumption such as the U.S. EPA
326 regulations ($2.0\mu\text{g/L}$) or the Spanish laws ($1.0\mu\text{g/L}$).

327 The detection limit obtained with this SPCNTnAuE sensor lower compared with other published works
328 where portable screen-printed electrodes are used as transducers for mercury determination in
329 water. Thus, Khaled et al.[48] obtained a $2.0\mu\text{g/L}$ detection limit using chitosan modified
330 SPCEs. Bernalte et al. achieved a detection limit of $1.1\mu\text{g/L}$ employing commercial gold screen-
331 printed electrodes[15] and $0.8\mu\text{g/L}$ using commercial gold nanostructured screen-printed carbon
332 electrodes[49]. Other authors such as Mandil et al.[34] and Laschi et al.[42] obtained, using gold
333 modified screen-printed carbon electrodes, 1.5 and $0.9\mu\text{g/L}$, respectively. Besides the lower detection
334 limit, the sensor developed in the present work is able to detect a concentration as low as $0.5\mu\text{g/L}$
335 while in the mentioned works the lowest concentration of the calibration plots is $2.5\mu\text{g/L}$. This is a
336 clear advantage because if a sample is contaminated with $1.0\mu\text{g/L}$ of mercury and therefore is above
337 the legal limits in some countries, the SPCNTnAuE sensor is able to detect it.

338 The possible interferences presented by Cu (II), Se (IV), Zn (II), Cd (II) and Pb (II) were studied to
339 evaluate the selectivity of the developed sensor (Fig. 5A). A solution of $10\mu\text{g/L}$ of mercury was
340 measured in presence of 100-fold concentration of the interfering metal. The results showed that the
341 measured signal for mercury was not statistically different in presence of these metals, indicating that
342 these metal ions do not interfere with the detection of mercury. The deposition potential applied to
343 produce the first UPD of mercury on gold is $+0.30\text{ V}$, this methodology is highly selective for mercury
344 because practically no other metal is reduced applying this potential.

345 To study the stability of the SPCNTnAuEs, several sensors were prepared and stored at room
346 temperature. A solution of $10\mu\text{g/L}$ of mercury was measured for different days of the fabrication. The
347 results obtained are shown in Fig. 5B. While the sensor lost part of the analytical signal measured in
348 the day of its fabrication, it holds the 85 % of the initial signal, which remains constant during the first
349 30 days.

350 3.4. Mercury analysis in tap water with SPCNTnAuEs

351 In order to evaluate the performance of the SPCNTnAuE sensor in real samples, an analysis of tap
352 and river water was carried out using the standard addition method. Mercury level was undetectable
353 because, in normal conditions, its concentration should be below the detection limit of the method.
354 Therefore, the samples were spiked with 1.0, 5.0, and 10.0 µg/L of mercury and were taken as the
355 problem samples.

356
357 Every sample was analyzed by triplicate and the results obtained are shown in Table 3. The recovery
358 yields for the river samples were, in general, lower than for the tap water samples. The more complex
359 matrix of the river samples may be the reason of this difference. The results obtained demonstrate
360 that the sensor developed in this work can be applied to the accurate determination of mercury in real
361 samples and the obtained results are in good agreement with the determination using ICP-MS as the
362 reference technique. A student's t-test, at a 95 % confidence level, showed no statistical difference
363 between both methods.

364 3.5. Analytical response for the simultaneous determination of lead and mercury

365 Lead is another metal that presents the underpotential deposition on gold electrodes and has been
366 determined using gold nanoparticles on screen-printed carbon electrodes[29]. In the same way as
367 mercury, the most interesting process is the first UPD. The first UPD of lead in HCl 0.1 M occurs at -
368 0.25 V[27]. Therefore, the separation between the first UPD for lead and mercury allows the
369 simultaneous electrochemical determination of both metals.

370 The ability of the developed sensor (SPCNTnAuE) for the simultaneous determination of lead and
371 mercury was evaluated. Calibration plots were obtained and are described by the following linear
372 regressions: $i (\mu\text{A}) = 2.766 + 0.203 \cdot [\text{Pb}^{2+}]$, and $i (\mu\text{A}) = 0.209 + 0.228 \cdot [\text{Hg}^{2+}]$, for lead and mercury,
373 respectively. These calibration plots showed a linear range of 2-100 µg/L and 2-60 µg/L with a limit of
374 detection of 2.0 and 1.9 µg/L for lead and mercury, respectively. Interelectrode reproducibility was
375 3.4% for lead and 4.1% for mercury.

376 The competition between lead and mercury for gold sites may be the main cause for obtaining a
377 detection limit for mercury not as low as in the case of the separate determination of mercury. The
378 results obtained demonstrate the possibility to fabricate a cheap, fast and low cost sensor for the
379 simultaneous determination of two toxic heavy metals at µg/L range of concentration.

380

381 4. Conclusions

382 The UPD process is a useful analytical tool for the electrochemical analysis of some metals, such as
383 mercury, on gold electrodes. Its behavior as an adsorption process, allows a more efficient
384 preconcentration of mercury on the electrode, and therefore a lower concentration can be detected.

385

386 Gold nanostructures allow the electrochemical determination of mercury with a good performance,
387 resulting in better sensitivity and better analytical characteristics than gold continuous surfaces or
388 conventional electrodes.

389

390 Moreover, if a nanohybrid material combining carbon nanotubes and gold nanoparticles is used as
391 electrode material, the characteristics of the method are significantly improved.

392

393 We used these excellent tools for the fabrication of an electrochemical sensor that allows a fast,
394 cheap, and easy analysis of mercury in water detecting concentrations below the legal limits. Due to
395 the portability of the instrumentation employed with screen-printed electrodes, the proposed method
396 could be used for in-situ measurements of environmental samples.

397

398 This work demonstrates that the modification of SPEs with nanohybrid materials is a wide open
399 window to explore for solving new analytical problems in a very simple way.

400

401 **References**

402

403 [1] E.G. Pacyna, J.M. Pacyna, F. Steenhuisen, S. Wilson, Global anthropogenic mercury
404 emission inventory for 2000, *Atmos. Environ.* 40 (2006) 4048–4063.

405 [2] Q. Wang, D. Kim, D.D. Dionysiou, G.A. Sorial, D. Timberlake, Sources and remediation for
406 mercury contamination in aquatic systems—a literature review, *Environ. Pollut.* 131 (2004)
407 323–336.

408 [3] N. Bloom, W.F. Fitzgerald, Determination of volatile mercury species at the picogram level by
409 low-temperature gas chromatography with cold-vapour atomic fluorescence detection, *Anal.*
410 *Chim. Acta.* 208 (1988) 151–161.

411 [4] J. Murphy, P. Jones, S.J. Hill, Determination of total mercury in environmental and biological
412 samples by flow injection cold vapour atomic absorption spectrometry, *Spectrochim. Acta, Part*
413 *B.* 51 (1996) 1867-1873.

414 [5] J.S. dos Santos, M. de la Guardia, A. Pastor, M.L.P. dos Santos, Determination of organic and
415 inorganic mercury species in water and sediment samples by HPLC on-line coupled with ICP-
416 MS, *Talanta.* 80 (2009) 207-11.

417 [6] EPA, Mercury in aqueous samples and extracts by anodic stripping voltammetry, Method
418 7472, n.d.

419 [7] J.-M. Zen, M.-J. Chung, Square-wave voltammetric stripping analysis of mercury(II) at a
420 poly(4-vinylpyridine)/gold film electrode, *Anal. Chem.* 67 (1995) 3571-3577.

421 [8] P. Salaün, C.M.G. van den Berg, Voltammetric detection of mercury and copper in seawater
422 using a gold microwire electrode, *Anal. Chem.* 78 (2006) 5052-60.

423 [9] E. Herrero, L.J. Buller, H.D. Abruña, Underpotential deposition at single crystal surfaces of Au,
424 Pt, Ag and other materials, *Chem. Rev.* 101 (2001) 1897-930.

- 425 [10] R.D. Riso, M. Waeles, P. Monbet, C.J. Chaumery, Measurements of trace concentrations of
426 mercury in sea water by stripping chronopotentiometry with gold disk electrode: influence of
427 copper, *Anal. Chim. Acta.* 410 (2000) 97-105.
- 428 [11] E. Viltchinskaia, L. Zeigman, D. Garcia, P. Santos, Simultaneous determination of mercury
429 and arsenic by anodic stripping voltammetry, *Electroanalysis.* 9 (1997) 633–640.
- 430 [12] O. Ordeig, C.E. Banks, J. del Campo, F.X. Muñoz, R.G. Compton, Trace Detection of Mercury
431 (II) Using Gold Ultra-Microelectrode Arrays, *Electroanalysis.* 18 (2006) 573-578.
- 432 [13] H. Huiliang, D. Jagner, L. Renman, Simultaneous determination of mercury (II), copper (II) and
433 bismuth (III) in urine by flow constant-current stripping analysis with a gold fibre electrode,
434 *Anal. Chim. Acta.* 202 (1987) 117–122.
- 435 [14] K.C. Honeychurch, J.P. Hart, Screen-printed electrochemical sensors for monitoring metal
436 pollutants, *TrAC, Trends Anal. Chem.* 22 (2003) 456-469.
- 437 [15] E. Bernalte, C. Marín Sánchez, E. Pinilla Gil, Determination of mercury in ambient water
438 samples by anodic stripping voltammetry on screen-printed gold electrodes, *Anal. Chim. Acta.*
439 689 (2011) 60-4.
- 440 [16] V. Meucci, S. Laschi, M. Minunni, C. Pretti, L. Intorre, G. Soldani, et al., An optimized digestion
441 method coupled to electrochemical sensor for the determination of Cd, Cu, Pb and Hg in fish
442 by square wave anodic stripping voltammetry, *Talanta.* 77 (2009) 1143-8.
- 443 [17] D. Hernández-Santos, M.B. González-García, A. Costa García, Metal-nanoparticles based
444 electroanalysis, *Electroanalysis.* 14 (2002) 1225–1235.
- 445 [18] F.W. Campbell, R.G. Compton, The use of nanoparticles in electroanalysis: an updated
446 review, *Anal. Bioanal. Chem.* 396 (2010) 241-59.
- 447 [19] M.T. Fernández-Abedul, A. Costa-García, Carbon nanotubes (CNTs)-based electroanalysis,
448 *Anal. Bioanal. Chem.* 390 (2008) 293–298.
- 449 [20] J.M. Pingarrón-Carrazón, P. Yáñez-Sedeño, A. González-Cortés, Gold nanoparticle-based
450 electrochemical biosensors, *Electrochim. Acta.* 53 (2008) 5848–5866.
- 451 [21] A. Merkoċi, M. Pumera, X. Llopis, B. Perez, M. Delvalle, S. Alegret, New materials for
452 electrochemical sensing VI: Carbon nanotubes, *TrAC, Trends Anal. Chem.* 24 (2005) 826-838.
- 453 [22] T. Kuila, S. Bose, P. Khanra, A.K. Mishra, N.H. Kim, J.H. Lee, Recent advances in graphene-
454 based biosensors, *Biosens. Bioelectron.* (2011).
- 455 [23] O. Abollino, A. Giacomino, M. Malandrino, G. Piscionieri, E. Mentasti, Determination of
456 Mercury by Anodic Stripping Voltammetry with a Gold Nanoparticle-Modified Glassy Carbon
457 Electrode, *Electroanalysis.* 20 (2008) 75–83.
- 458 [24] H. Yi, Anodic stripping voltammetric determination of mercury using multi-walled carbon
459 nanotubes film coated glassy carbon electrode, *Anal. Bioanal. Chem.* 377 (2003) 770-4.
- 460 [25] H. Xu, L. Zeng, S. Xing, G. Shi, Y. Xian, L. Jin, Microwave-radiated synthesis of gold
461 nanoparticles/carbon nanotubes composites and its application to voltammetric detection of
462 trace mercury(II), *Electrochem. Commun.* 10 (2008) 1839-1843.
- 463 [26] J. Gong, T. Zhou, D. Song, L. Zhang, Monodispersed Au nanoparticles decorated graphene as
464 an enhanced sensing platform for ultrasensitive stripping voltammetric detection of mercury(II),
465 *Sens. Actuators, B.* 150 (2010) 491-497.

- 466 [27] G. Martínez-Paredes, M.B. González-García, A. Costa-García, In situ electrochemical
467 generation of gold nanostructured screen-printed carbon electrodes. Application to the
468 detection of lead underpotential deposition, *Electrochim. Acta.* 54 (2009) 4801–4808.
- 469 [28] P. Fanjul-Bolado, P. Queipo, P.J. Lamas-Ardisana, A. Costa-García, Manufacture and
470 evaluation of carbon nanotube modified screen-printed electrodes as electrochemical tools,
471 *Talanta.* 74 (2007) 427-33.
- 472 [29] G. Martínez-Paredes, M.B. González-García, A. Costa-García, Lead Sensor Using Gold
473 Nanostructured Screen-Printed Carbon Electrodes as Transducers, *Electroanalysis.* 21 (2009)
474 925–930.
- 475 [30] G. Liu, Y. Lin, Voltammetric detection of Cr(VI) with disposable screen-printed electrode
476 modified with gold nanoparticles, *Environ. Sci. Technol.* 42 (2008) 3117.
- 477 [31] G. Martínez-Paredes, M.B. González-García, A. Costa-García, Genosensor for SARS Virus
478 Detection Based on Gold Nanostructured Screen-Printed Carbon Electrodes, *Electroanalysis.*
479 21 (2009) 379-385.
- 480 [32] G. Martínez-Paredes, M.B. González-García, A. Costa-García, Genosensor for detection of
481 four pneumoniae bacteria using gold nanostructured screen-printed carbon electrodes as
482 transducers, *Sens. Actuators, B.* 149 (2010) 329-335.
- 483 [33] P.J. Lamas-Ardisana, P. Queipo, P. Fanjul-Bolado, A. Costa-García, Multiwalled carbon
484 nanotube modified screen-printed electrodes for the detection of p-aminophenol: Optimisation
485 and application in alkaline phosphatase-based assays, *Anal. Chim. Acta.* 615 (2008) 30–38.
- 486 [34] A. Mandil, L. Idrissi, A. Amine, Stripping voltammetric determination of mercury(II) and lead(II)
487 using screen-printed electrodes modified with gold films, and metal ion preconcentration with
488 thiol-modified magnetic particles, *Microchim. Acta.* 170 (2010) 299-305.
- 489 [35] M.M. Pereira da Silva Neves, M.B. González-García, C. Delerue-Matos, A. Costa-García,
490 Nanohybrid Materials as Transducer Surfaces for Electrochemical Sensing Applications,
491 *Electroanalysis.* 23 (2011) 63–71.
- 492 [36] M.M.P.S. Neves, M.B. González-García, H.P.A. Nouws, A. Costa-García, Celiac disease
493 detection using a transglutaminase electrochemical immunosensor fabricated on nanohybrid
494 screen-printed carbon electrodes, *Biosens. Bioelectron.* In Press (2011).
- 495 [37] C.M. Welch, O. Nekrassova, X. Dai, M.E. Hyde, R.G. Compton, Fabrication, characterisation
496 and voltammetric studies of gold amalgam nanoparticle modified electrodes, *ChemPhysChem.*
497 5 (2004) 1405–1410.
- 498 [38] E. Herrero, H.D. Abruña, Underpotential Deposition of Mercury on Au(111): Electrochemical
499 Studies and Comparison with Structural Investigations, *Langmuir.* 13 (1997) 4446-4453.
- 500 [39] J. Li, E. Herrero, H.D. Abruña, The effects of anions on the underpotential deposition of Hg on
501 Au (111) An electrochemical and in situ surface X-ray diffraction study, *Colloids Surf., A.* 134
502 (1998) 113–131.
- 503 [40] J. Li, H.D. Abruña, Phases of Underpotentially Deposited Hg on Au(111): An in Situ Surface X-
504 ray Diffraction Study, *J. Phys. Chem. B.* 101 (1997) 2907-2916.
- 505 [41] A. Giacomino, O. Abollino, M. Malandrino, E. Mentasti, Parameters affecting the determination
506 of mercury by anodic stripping voltammetry using a gold electrode, *Talanta.* 75 (2008) 266-73.

- 507 [42] S. Laschi, I. Palchetti, M. Mascini, Gold-based screen-printed sensor for detection of trace
508 lead, *Sens. Actuators, B.* 114 (2006) 460-465.
- 509 [43] X. Yang, In-situ atomic force microscope observation of stripping of mercury from Hg/Au alloy
510 films in acidic media, *Surf. Sci.* 324 (1995) L363-L366.
- 511 [44] L.E. Barrosse-Antle, L. Xiao, G.G. Wildgoose, R. Baron, C.J. Salter, A. Crossley, et al., The
512 expansion/contraction of gold microparticles during voltammetrically induced amalgamation
513 leads to mechanical instability, *New J. Chem.* 31 (2007) 2071.
- 514 [45] J. Wang, D. Larson, N. Foster, S. Armalis, J. Lu, X. Rongrong, et al., Remote electrochemical
515 sensor for trace metal contaminants, *Anal. Chem.* 67 (1995) 1481-1485.
- 516 [46] J. Inukai, S. Sugita, K. Itaya, Underpotential deposition of mercury on Au(111) investigated by
517 in situ scanning tunnelling microscopy, *J. Electroanal. Chem.* 403 (1996) 159-168.
- 518 [47] W.H. Organization, Guidelines for drinking-water quality, Fourth, Geneva, 2011.
- 519 [48] E. Khaled, H. Hassan, I. Habib, Chitosan Modified Screen-Printed Carbon Electrode for
520 Sensitive Analysis of Heavy Metals, *Int. J. Electrochem.* 5 (2010) 158-167.
- 521 [49] E. Bernalte, C.M. Sánchez, E.P. Gil, Gold Nanoparticles-Modified Screen-Printed Carbon
522 Electrodes For Anodic Stripping Voltammetric Determination Of Mercury In Ambient Water
523 Samples, *Sens. Actuators, B.* In Press (2011).

524

525

526 **Biographies**

527 **Daniel Martín-Yerga** obtained her B.Sc. degree in chemistry, focus on analytical chemistry in 2010
528 (University of Oviedo) and the M.Sc. degree in analytical and bioanalytical chemistry in 2011
529 (University of Oviedo). At present, he is collaborating with the Immunoanalytical Research
530 Group of the University of Oviedo, supervised by Prof. A. Costa-García.

531 **MaríaBegoña González-García** obtained her B.Sc. degree in chemistry, focus in analytical
532 chemistry, in 1991 (University of Oviedo) and the Ph.D. in chemistry in 1999 (University of Oviedo).
533 Nowadays she is working as associated professor at the University of Oviedo and is a co-worker in
534 the Immunoanalytical Research Group of the same university, supervised by Prof. A. Costa-
535 García.

536 **Agustín Costa-García** obtained his B.Sc. degree in chemistry, focus in analytical chemistry, in 1974
537 (University of Oviedo) and the Ph.D. in chemistry in 1977 (University of Oviedo). Since February 2000
538 he is professor in analytical chemistry (University of Oviedo). He leads the Immunoanalytical
539 Research Group of the University of Oviedo and has been supervisor of several research projects
540 developed at the electrochemistry laboratories of the Department of Physical and Analytical
541 Chemistry of the University of Oviedo. Nowadays his research is focused on the development of

542 nanostructured electrodic surfaces and its use as transducers for electrochemical immunosensors
543 and genosensors employing both enzymatic and non-enzymatic labels.

544 **Captions of Tables**

545

546 **Table 1:** Mean diameter of the gold nanoparticles and amount of gold deposited on the different
547 electrode surfaces. The value of mean diameter written with bold letters corresponds to the group with
548 greater number of nanoparticles.

549

550 **Table 2:** Analytical characteristics obtained for different nanostructured sensors.

551

552 **Table 3:** Mercury determination in tap and river water samples using SPCNTnAuEs and ICP-MS after
553 spiking with 1, 5 and 10 $\mu\text{g/L}$ of mercury.

554

555 **Captions of Figures**

556

557 **Figure 1:** Cyclic voltammograms for 500 mg/L of mercury (continuous line) and blank solution
558 (dashed line) for SPCEs (A), SPAuEs (B) and SPCnAuEs (C) in HCl 0.10 M. Scan rate: 100 mV/s.

559

560 **Figure 2:**(A) Cyclic voltammograms at potentials near the first UPD for 100 mg/L of mercury for
561 SPCnAuEs (continuous line) and SPAuEs (dashed line). (B) Cyclic voltammograms for 5 mg/L
562 (continuous line) and 250 $\mu\text{g/L}$ (dashed line) of mercury, after deposition at 0.10 V during 60 s using
563 SPCnAuEs. Scan rate: 100 mV/s. Supporting electrolyte: HCl 0.10 M.

564

565 **Figure 3:** SEM images of SPCnAuE (A), SPCNTnAuE (B) and SPGOnAuE (C). Magnification factor:
566 1×10^4 .

567

568 **Figure 4:** Calibration plot and square-wave voltammograms (after baseline correction
569 method) obtained using SPCNTnAuEs for 0.5, 1, 2, 5, 10, 20, 40 and 50 $\mu\text{g/L}$ of mercury in HCl 0.10
570 M. See Table 2 for experimental parameters. Deposition potential: +0.30 V.

571

572 **Figure 5:**(A) Effects of various metal ions on the analytical signal of Hg(II) using SPCNTnAuEs.
573 Mercury concentration: 10 $\mu\text{g/L}$. Metal concentration: 10 mg/L. (B) Stability of the mercury
574 SPCNTnAuE sensor for a month. Mercury concentration: 10 $\mu\text{g/L}$. Supporting electrolyte: HCl 0.10 M.

575

576

576
577
578
579

Table 1

	Diameter (nm)	Mass Au (ng)
SPCnAuEs	135 ± 16	(1.28 ± 0.08) × 10 ²
SPGOnAuEs	298 ± 35 154 ± 33 90 ± 10	(8.4 ± 0.9) × 10 ²
SPCNTnAuEs	148 ± 12 87 ± 10	(9.0 ± 0.8) × 10 ²

580
581
582

582

583

584

Table 2

	Linear range ($\mu\text{g/L}$)	Slope ($\mu\text{A}\cdot\text{L}/\mu\text{g}$)	R^2	DL ($\mu\text{g/L}$)	RSD (%) ¹
SPCnAuEs	5-100	0.120	0.996	3.3	7.3
SPGOnAuEs	2-50	0.082	0.996	1.9	16.4
SPCNTnAuEs	0.5-50	0.237	0.9998	0.2	3.0

585 ¹ Reproducibility obtained for five electrodes

586

587

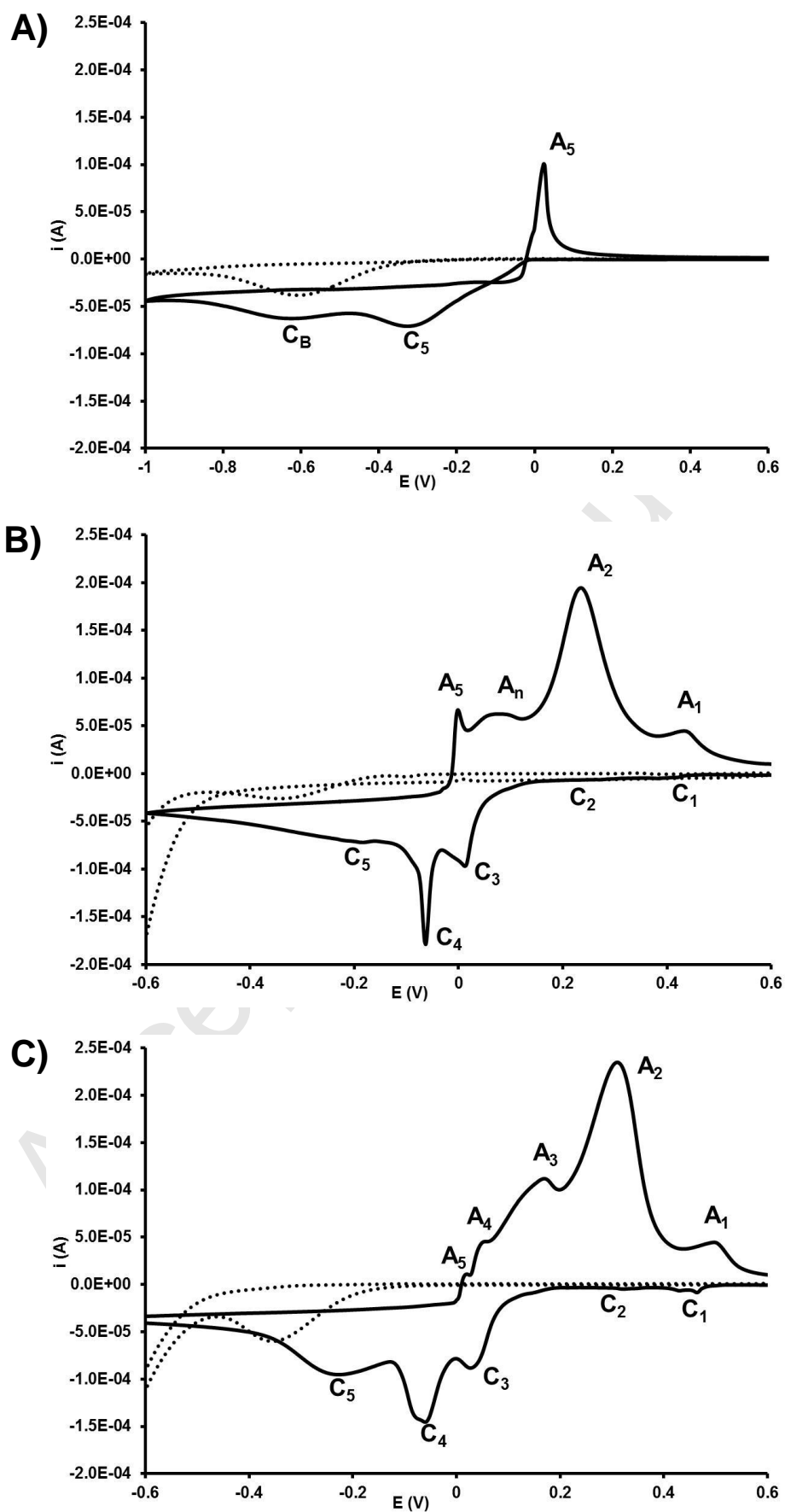
588

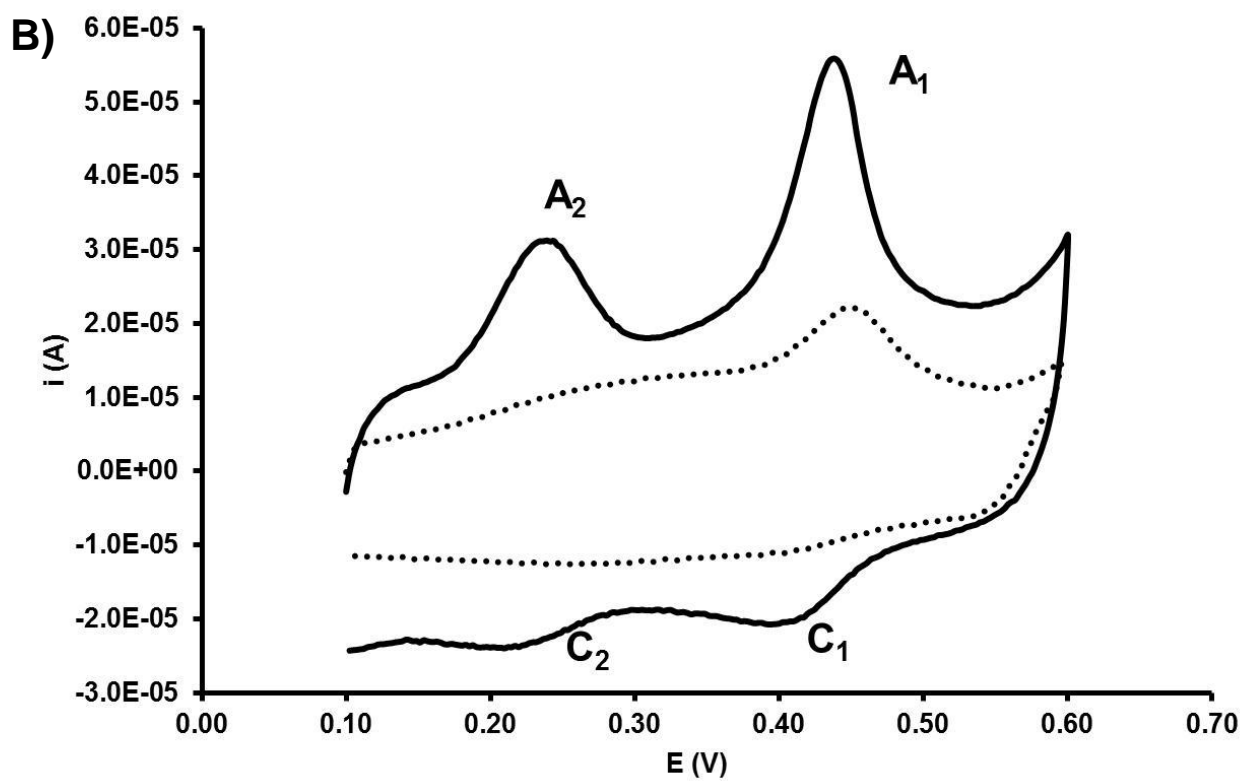
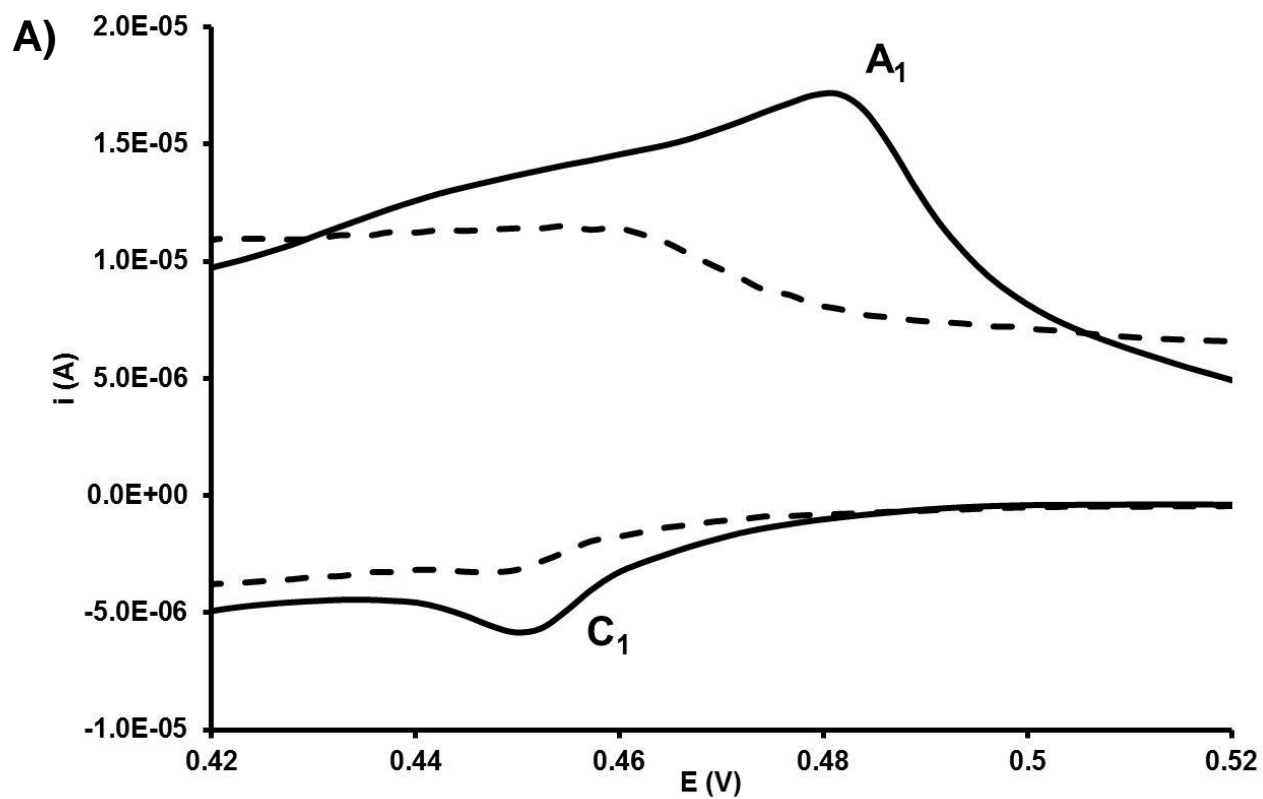
588
589
590
591

Table 3

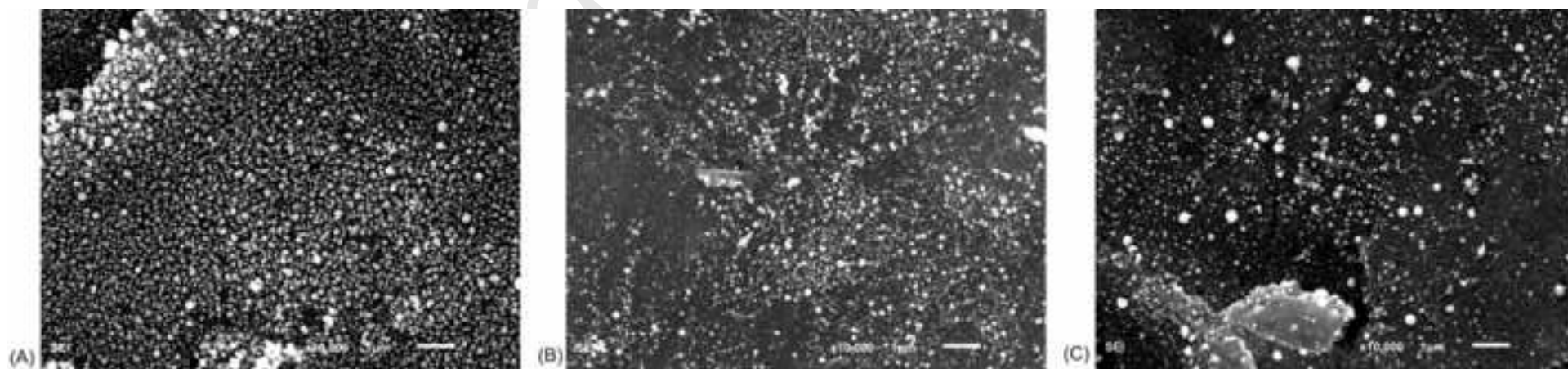
	Added ($\mu\text{g/L}$)	Found ($\mu\text{g/L}$)	Recovery (%)	ICP-MS ($\mu\text{g/L}$)
Tap water	1	1.03 ± 0.07	95.3-108.3	0.98 ± 0.02
	5	4.9 ± 0.4	91.0-106.2	5.4 ± 0.2
	10	10.3 ± 0.8	95.7-111.5	10.6 ± 0.1
River water	1	0.8 ± 0.1	68.0-92.4	0.61 ± 0.04
	5	3.8 ± 0.4	70.6-83.8	3.80 ± 0.05
	10	7.7 ± 0.8	71.1-82.1	7.1 ± 0.2

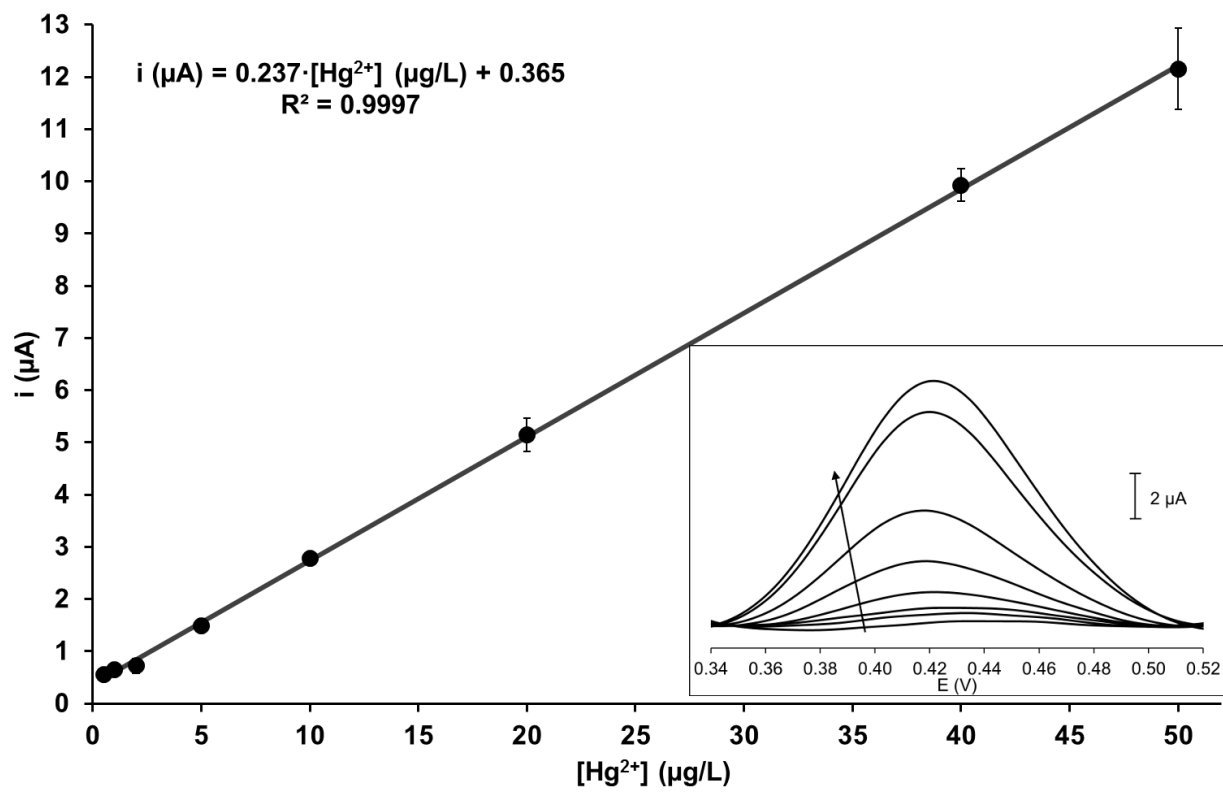
592
593





Manuscript





Accepted

